

TO THE FINAL STATE OF RECTANGULAR FRAMES

by
Ryo Tanabashi*, Kiyoshi Kaneta*, Tsuneyoshi Nakamura# and Shuzo Ishida†

Abstract

The senior author, R. Tanabashi proposed the "Velocity-Potential Energy Theory" in 1935 [1]. The theory maintains that the effective intensity of the ground motion due to an earthquake disturbance acting upon a structure is proportional to the square of the maximum velocity and that the resistance of the structure against the earthquake is governed by the potential energy that the structure can store before it collapses. Since then, the senior author has continuously insisted on the importance of this energy absorption capacity as one of the most significant measures representing the overall earthquake resistance of a structure. The theory has been reconfirmed for a bilinear hysteretic multi-degree-of-freedom system by T. Kobori and R. Minai [2].

The purpose of the present paper is to reveal characteristics of energy absorption capacities of ten & five-story frames. The following conclusions are drawn from the numerical results on 39 elastic-perfectly plastic unbraced frames subjected to proportional horizontal loads under constant vertical loads.

- (1) Frames with relatively strong columns and weak beams exhibit rather stable static responses in the sense that the load-displacement response curves are essentially of bilinear elastic-perfectly plastic type without portions of large negative slopes. An overturning moment-overall rotation curve of bilinear elastic-perfectly plastic type is characterized by a constant average rate of work done by the horizontal forces which is nothing but an energetic representation of the average overall strength.
- (2) The plastic hinge rotation is almost linear with respect to the top displacement as in a rigid-plastic collapse mechanism. The displacement limit or the overall rotation limit may be determined from the rotation capacities of plastic hinges in a frame and may be used to define the final state.
- (3) A frame with a greater rate of linear tapering in beam sections per story toward top has a greater energy absorption capacity even if the sum of beam plastic moments are the same.
- (4) The average rate of energy absorption W_H' is proportional to the magnitude of beam plastic moments, whereas the W_H' -value increases with respect to the rate of tapering at a considerably smaller rate than with respect to the rate of increase in the plastic moments. A frame with greater plastic moments has a greater energy absorption capacity.
- (5) Patterns of horizontal load distributions have only slight influence upon the energy absorption capacity.
- (6) Five-story frames of two bays exhibit similar behaviors to those of ten-story frames of one bay, except that the overturning moment-overall rotation curves do not have any portions of even slight negative slopes.

* Professor of Architecture, Kyoto University, Kyoto, Japan

Assistant Professor of Architecture, Kyoto University

† Assistant Professor of Civil Engineering, Ritsumeikan University

[1] R. Tanabashi, "Some Considerations on Destructive Elements of Earthquake Ground Motion and Earthquake Resistance of Structures", Journal of the Architectural Institute of Japan, Vol.49, No.599, May 1935

[2] T. Kobori and R. Minai, "Aseismic Design Method of Elasto-plastic Building Structures", Disaster Prevention Research Institute, Kyoto University, Bulletin No.68, March 1964.

Ryo Tanabashi¹⁾
 Kiyoshi Kaneta²⁾
 Tsuneyoshi Nakamura³⁾
 Shuzo Ishida⁴⁾

Synopsis

The senior author, R. Tanabashi, has insisted on the importance of the total energy absorption capacity of a structural system as one of the most significant intrinsic measures representing the overall earthquake resistance of the system. In this paper, the energy absorption capacities of 39 elastic-perfectly plastic unbraced rectangular frames of two different types subjected to proportional horizontal loads under constant vertical loads are investigated by a static numerical analysis. The numerical results reveal how the energy absorption capacity of a frame is influenced by the magnitudes and distributions of flexural stiffnesses and fully plastic moments and by the distribution of horizontal loads.

1. INTRODUCTION

The dynamic response analysis of a framed structure subjected to the ground-motion excited by a strong earthquake not only is quite complicated due to the inherently nonlinear behavior of the structure, but also requires probabilistic techniques due to the uncertainty and random nature of the earthquake disturbances. Under such a circumstance, it is a meaningful and practically important effort to seek for an intrinsic measure representing the overall earthquake resistance of a framed structure.

The senior author, R. Tanabashi proposed the "Velocity-Potential Energy Theory" in 1935 [1]. The theory maintains that the effective intensity of the ground motion due to an earthquake disturbance acting upon a structure is proportional to the square of the maximum velocity and that the resistance of the structure against the earthquake is governed by the potential energy that the structure can store before it collapses. Since then, the senior author has continuously insisted on the importance of this energy absorption capacity as one of the most significant measures representing the overall earthquake resistance of a frame. Although the theory was illustrated only for a one-degree-of-freedom system in the 1935 paper, other investigators have also taken similar approaches [2], indicating the acceptance of the theory. T. Kobori and R. Minai have shown recently that, although a bilinear hysteretic multi-degree-of-freedom system subjected to strong motion earthquakes behaves in a complicated manner exhibiting hysteretic cycles and dissipating energy, the energy required for the system to absorb per unit weight within certain

- 1), 2) Professors of Architecture, Kyoto University, Kyoto, Japan
 3) Assistant Professor of Architecture, Kyoto University
 4) Assistant Professor of Civil Engineering, Ritsumeikan University, Kyoto

allowable limits on its displacements is indeed proportional to the square of the maximum of a certain equivalent velocity belonging to an earthquake disturbance, but does not depend on the number of stories and the period characteristics. [3]

A highly statically indeterminate structure consisting of ductile materials can absorb a large amount of energy before it collapses due to external disturbances. Quantitative estimates of the energy capacities of tall multi-story frames have, however, been very few and how the energy capacity of a frame is influenced by the stiffnesses and strengths of the members has not been investigated at all.

This paper presents the results of an extensive static numerical analysis of 39 elastic-perfectly plastic unbraced rectangular frames of two different types subjected to proportional horizontal loads under constant vertical loads. The numerical results reveal certain characteristics of energy absorption capacities of the frames. It is investigated how the energy absorption capacity of a tall multi-story frame is influenced by the magnitudes and distributions of flexural stiffnesses and fully plastic moments and by the distribution of horizontal loads. Fig.1 shows two types of frames considered here.

The present analysis is based upon the following assumptions.

- (1) An unbraced rectangular frame with the common plane of symmetry for all the members is subjected to quasi-static loads within the plane of symmetry. Out-of-plane deformation is prevented. Local deformation within a cross-section such as flange buckling is not taken into consideration.
- (2) Corresponding to the idealization of a member to a one-dimensional object with a uniform flexural stiffness, a joint is also idealized to be a point at which all the members in contact are rigidly connected.
- (3) The magnitudes of horizontal loads assumed to be acting only upon floor levels are specified by a load factor. All the dead and live loads transmitted to the frame can be replaced by the four concentrated loads as shown in Fig.1. The magnitudes and distributions may be regarded as the same for all the girders throughout a frame and are constant during horizontal loading.
- (4) Horizontal displacements due to bending deformation are finite but small so that terms higher than the second order can be neglected. Shear and axial deformations in members and joints are neglected.
- (5) The moment-curvature relation for a cross-section of a beam is elastic-perfectly plastic. Strain-hardening effect is not taken into consideration.
- (6) Since a plastic hinge formed in a column subjected to a large axial force induces undesirable unstable plastic behavior of the column especially under cyclic lateral loading, the present analysis is confined to those frames so designed that all the columns remain elastic during horizontal loading. This assumption is seen to be satisfied a posteriori in most cases considered here so far as displacements are not very large. [4]

2. STIFFNESS MATRIX METHOD FOR SECOND-ORDER ELASTIC-PLASTIC ANALYSIS

The stiffness matrix method has many advantages for analysis of complex structures consisting of a great number of members. The compactness in representing the diversified structural characteristics of a complex system and the automatic procedure of composing the system stiffness matrix from individual member stiffness matrices make the method computer oriented. A system stiffness matrix for second-order elastic-plastic analysis is characterized by the fact that it is a function of axial forces in columns and by the circumstance that it depends upon the state of plastic hinge formation.

Hence an elastic-plastic response analysis is necessarily of an incremental nature.

Since all the columns of a frame have been assumed to remain elastic within the range of static response under consideration, the well-known member stiffness matrix which takes into account the reduction of its flexural stiffness due to the axial compression [5] may be used. For a column of length with flexural stiffness EI subjected to an axial compression N, the member stiffness matrix may be written as

$$\begin{bmatrix} \frac{12\psi}{4\psi^2 - \phi^2} \frac{EI}{l} & \frac{6\phi}{4\psi^2 - \phi^2} \frac{EI}{l} & -\frac{6}{2\psi - \phi} \frac{EI}{l^2} \\ \frac{6\phi}{4\psi^2 - \phi^2} \frac{EI}{l} & \frac{12\psi}{4\psi^2 - \phi^2} \frac{EI}{l} & -\frac{6}{2\psi - \phi} \frac{EI}{l^2} \\ -\frac{6}{2\psi - \phi} \frac{EI}{l^2} & -\frac{6}{2\psi - \phi} \frac{EI}{l^2} & \left[\frac{12}{2\psi - \phi} - \eta^2 \right] \frac{EI}{l^3} \end{bmatrix} \quad (1)$$

where

$$\eta = \sqrt{\frac{Nl^2}{EI}}, \quad \psi(\eta) = \frac{3}{\eta} \left(\frac{1}{\eta} - \frac{1}{\tanh\eta} \right) \quad \text{and} \quad \phi(\eta) = \frac{6}{\eta} \left(\frac{1}{\sin\eta} - \frac{1}{\eta} \right) \quad (2)$$

It should be noted that the effect of the additional moment due to the axial compression on the sway stiffness has been included in the last element. As the axial compression in a column varies corresponding to the increase of horizontal loads, the elements of the stiffness matrix must be computed for every step of the incremental procedure described later. For a column subjected to axial tension in the process of large sway deflection, a similar stiffness matrix containing hyperbolic functions is used [5].

Since elongations in beams and columns have been assumed to be negligible, the angle of rotation at the ends of a beam may only be taken as the independent coordinates for the beam. As far as a beam remains elastic, the well-known member stiffness matrix may be used. If a plastic hinge forms at a cross-section of the beam, the flexural stiffness for the subsequent incremental bending in the direction of the plastic hinge rotation is reduced considerably and the corresponding new stiffness matrix must be used instead. If the direction of the plastic hinge rotation is to be reversed at a later step, then the elastic stiffness matrix must again be used. The difficulty here is that, due to this possibility of reversal in hinge rotation, whether the member stiffness matrix used for an incremental step has been appropriate or not depends upon the resulting incremental angles of end rotation and consequently resulting incremental hinge rotation. Whether the angle of hinge rotation increases or decreases must always be judged only from the result a posteriori. This is the difficulty inherent to most problems in plasticity.

In view of the assumed locations of the concentrated loads on a beam, there are four potentially critical sections where a plastic hinge may form. Fig.2 shows six different possibilities of plastic hinge formation. A one-hinge pattern and three cases of two-hinge patterns have been excluded here since it is known a priori that those cases can not occur under monotonically increasing horizontal loads from left in view of the moment distribution shown in Fig.2(a). As far as the plastic hinge rotation proceeds in the three one-hinge patterns shown in Fig.2(b),(c) and (d), the member stiffness matrix may be compactly written as

$$\begin{bmatrix} \frac{3EI}{l} & \frac{r^2}{3r^2-3r+1} & \frac{3EI}{l} & \frac{r(1-r)}{3r^2-3r+1} \\ \frac{3EI}{l} & \frac{r(1-r)}{3r^2-3r+1} & \frac{3EI}{l} & \frac{(1-r)^2}{3r^2-3r+1} \end{bmatrix} \quad (3)$$

where $r = 0, 1/3$ and 1 for (b), (c) and (d), respectively. Depending upon the combinations of the incremental angles of end rotation, the stiffness matrix for a two-hinge pattern shown in Fig.2(e), (f) or (g) may be either the elastic stiffness matrix, the null matrix or reduced to one of those for one-hinge patterns.

If all the member stiffness matrices are known, then the system stiffness matrix may readily be constructed in accordance with the reference coordinate system chosen for a frame. The code system [6] has been employed in the present analysis in a modified form.

3. COMPUTATIONAL PROCEDURE

Since the system stiffness of a frame is changed whenever a new plastic hinge forms or disappears, the elastic-plastic response analysis must be carried out in an incremental form. The additional moments induced by the horizontal sway displacements under large vertical loads are taken into account in the present second-order analysis and may result in a load factor-displacement curve with a negative slope. This circumstance indicates that a load increment, if taken as an independent variable, will cause certain difficulties in the vicinity of the point of the largest load factor. Hence a displacement increment has been chosen as the independent variable here.

The computational procedure employed here may be summarized as follows.

- (1) Form the elastic system stiffness equation for a frame based upon the initial axial forces in the columns due to the vertical loads only. Solve the set of simultaneous linear algebraic equations for equivalent joint forces due to vertical loads only. Superpose fixed beam moment distribution on the result obtained above. Store all the response quantities including bending moments $M_i^{(0)}$ at all the potentially critical sections of the beams.
- (2) Solve the same set of simultaneous linear algebraic equation for a unit relative displacement at the top story of the frame. Find the value of the displacement multiplier $y_m^{(0)}$ at which the bending moment at a cross-section attains its fully plastic moment, while other sections remain within or at their respective fully plastic moments. In other words, find

$$y_m^{(0)} = \min \{ y_i^{(0)} \} \quad \text{among } y_i^{(0)} \text{ such that } M_i^{(0)} + y_i^{(0)} M_i^{(0)} = M_{ip}$$

where M_{ip} denotes the fully plastic moment of section i in the positive direction of end moments or cross-sectional bending moments. Compute the response quantities for this displacement increment $y_m^{(0)}$ by multiplying those for a unit relative displacement by $y_m^{(0)}$.

- (3) The member stiffness matrix for a beam containing the section m must be replaced by the plastic one described in the preceding section if the subsequent response is such that the plastic hinge rotation proceeds. Recompute also all the member stiffness matrices for the columns based upon the new values of axial forces obtained at the end of the second step. Based upon these new member stiffness matrices for beams and columns, synthesize the new system stiffness matrix.
- (4) Compute the response quantities including $M_i^{(2)}$ for a unit displacement. Check if the angle of rotation in the plastic hinge increases in the direction of the moment acting upon that section. If not, replace the plastic

member stiffness matrix by the elastic one and recompute the response quantities. Then go to (3).

- (5) If the plastic hinge rotation proceeds, then the moment increment at that section is zero, whereas moments at other sections vary. Find the value of the displacement multiplier increment at which the bending moment at a cross-section other than m attains its fully plastic moment, other sections remaining within or at their respective fully plastic moments. In other words, find

$$y_n^{(2)} = \min \{ y_j^{(2)} \} \quad \text{among } y_j^{(2)} \text{ such that } M_j^{(0)} + y_m^{(1)} M_j^{(1)} + y_j^{(2)} M_j^{(2)} = M_{ip}$$

Compute the response quantities for this displacement increment $y_n^{(2)}$ by

$$\bar{\chi}_j^{(2)} = y_m^{(1)} \chi_j^{(1)} + y_n^{(2)} \chi_j^{(2)}$$

- (6) Repeat the procedures (3) - (5) based upon the subsequent new plastic hinges until the frame is reduced to a kinematic mechanism consisting of at least twice as many plastic hinges as the number of beams.

4. STRUCTURAL DATA OF THE FRAMES CONSIDERED

The dimensions of the frames and the patterns of loading considered are shown in Fig. 1. Table 1 illustrates the parameters chosen as the basic variables for the eight series of frames. Let \bar{M}_p and \bar{I} denote the standard fully plastic moment and cross-sectional moment of inertia, respectively, in terms of which all the parameters are varied. The following values have been used for the present frames.

$$\begin{aligned} \bar{M}_p^K &= 9000 \text{ t cm}, & \bar{I}_B^K &= 93800 \text{ cm}^4, & \bar{I}_C^K &= 187600 \text{ cm}^4, \\ \bar{M}_p^U &= 6000 \text{ t cm}, & \bar{I}_B^U &= 62500 \text{ cm}^4, & \bar{I}_C^U &= 125000 \text{ cm}^4. \end{aligned}$$

The superscripts K and U refer to the K-series of ten-story frames of one bay and the U-series of five-story frames of two bays, respectively. The subscripts B and C refer to beam and column, respectively.

Frames of KAA-series are characterized by the following properties:

- (i) $\sum_i M_{ip}^{(j)}$ = constant through $j=1, 2, 3, 4, 5$ for KAA- j , so that they have a common mechanism curve if their collapse mechanisms are the same, (ii) The plastic moment $M_{ip}^{(j)}$ of the i -th story beam in the frame KAA- j is represented by

$$M_{ip}^{(j)} = \bar{M}_p^K \left\{ 1 + (i-5)(j-1) \frac{\Delta M_p}{\bar{M}_p^K} \right\} = \bar{M}_p^K \left\{ 1 + (i-5) r_T^{(j)} \right\} \quad (4)$$

where ΔM_p denotes the smallest increment in the linearly tapered plastic moments \bar{M}_p^K and where $(j-1) \frac{\Delta M_p}{\bar{M}_p^K} = r_T^{(j)}$ is called the rate of linear tapering (per story) in plastic moments, (iii) The stiffnesses of beams and columns are also linearly tapered toward top in the same manner as Eq. (4).

All the frames in KAB-series have the same column stiffness distribution as that of KAA-1. The other properties and the series parameter $r_T^{(j)}$ are the same as of KAA-series. In KAC-series, the stiffness $c_{KG} \bar{I}_B$ of the ground floor beam has been chosen as the series parameter, while other structural data are all the same as of KAA-1.

Frames of KBA-series and KBB-series have the same beam and column stiffnesses as those of KAA-1 and KAA-5, respectively. The magnitude of their distributed plastic moments is taken as the series parameter in both series as follows:

$$M_{ip}^{(j)} = c_M^{(j)} \bar{M}_p^K, \quad \text{where } c_M^{(j)} = (j+1)/4 \quad \text{for KBa-j frame} \quad (5),$$

$$M_{ip}^{(j)} = c_M^{(j)} \bar{M}_p^K \{ 1 + (i-5)r_T^{(5)} \} \quad \text{for KBb-j frame} \quad (6).$$

The corresponding mechanism curves in both series are translated with the same negative slope as far as the collapse mechanisms are the same. In KBC-series, the plastic moment $c_M \bar{M}_p$ of the ground floor beam is taken as the series parameter, while all the other structural data are the same as of KAA-1.

Frames of UAA-series have the same properties as those of KAA-series except that Eq. (4) must now be replaced by

$$M_{ip}^{(j)} = \bar{M}_p^U \{ 1 + (i - 2.5)(j-1) \Delta M_p / \bar{M}_p^U \} = \bar{M}_p^U \{ 1 + (i-2.5)r_T^{(j)} \} \quad (7)$$

Frames of UBA-series have the same beam and column stiffnesses as those of UAA-1. The magnitude of the uniformly distributed plastic moments is chosen as the series parameter as follows:

$$M_{ip}^{(j)} = c_M^{(j)} \bar{M}_p^U, \quad \text{where } c_M^{(j)} = (j+1)/4 \quad \text{for UBA-j frame} \quad (8)$$

5. NUMERICAL RESULTS

5.1 Static Response Quantities

In order to represent energy capacities and other static characteristics of the frames subjected to computer analysis, the following quantities were chosen for outputs. If the overturning moment M_{OVT} of the horizontal forces with respect to the ground is plotted with respect to θ_{ST} , the top horizontal displacement divided by the overall height of a frame, then the work done by the horizontal forces acting upon its plastic collapse mechanism is precisely represented by the area under the mechanism curve and the work done by the horizontal forces acting upon the elastic-perfectly plastic frame may roughly be represented by the area under the static response curve. In order to define a total energy absorption capacity of a frame, a final state or a limit on the displacements must first be determined. Such a limit may structurally be due to the rotation capacities of plastic hinges in the frame, or due to the deformation limits of non-structural components. It is therefore necessary to find the relation between θ_{ST} and the magnitudes of plastic hinge rotation. It is noted here that the same hinge may not necessarily always be the maximum as θ_{ST} increases. Therefore only for that hinge which attains the maximum angle of rotation at the last hinge point, the angle of rotation θ_p is plotted with respect to θ_{ST} .

As the energy quantity relevant to the kinetic energy, the work W_H done by the horizontal loads has been chosen for an output quantity with respect to θ_{ST} . Due to the presence of the vertical loads, the work W_H is not equal to the total energy E_T absorbed during deformation as illustrated in Fig.3. Although W_H consists of a substantial portion of the dissipated energy D_p and the elastic energy stored E_s so far as the displacements are finite but small, the internal energy is dissipated also for the work W_V done by the vertical loads. Since a W_H - θ_{ST} curve is almost linear after the formation of several plastic hinges as may be seen from Fig.6-1 ~8, it is meaningful to define the average rate of work W_H' done by the horizontal forces. The implication of W_H' is, in essence, an energetic representation of the average strength if an M_{OVT} - θ_{ST} curve is roughly regarded as an elastic-perfectly plastic bilinear response.

5.2 $M_{OVT} - \theta_{ST}$ curves

The $M_{OVT} - \theta_{ST}$ curves have been drawn under the respective mechanism curves in Fig. 4-1-8. The symbols \square and ∇ in the figures and in Table 1 indicate uniformly distributed and triangularly distributed loads, respectively. In KAA-series, an $M_{OVT} - \theta_{ST}$ curve for a frame with a greater rate of tapering in the stiffness and strength distributions attains a higher maximum and approaches its mechanism curve more closely from below at an earlier stage of deformation but the almost flat portion of the curve up to the last hinge point is smaller. The uniformly and triangularly distributed loads do not result in any substantial difference as far as the $M_{OVT} - \theta_{ST}$ relation is concerned. The $M_{OVT} - \theta_{ST}$ curves for KAB-j frames are almost the same as for KAA-j frames, respectively. This indicates that the linear tapering in column stiffnesses has only slight influence upon the $M_{OVT} - \theta_{ST}$ curves.

The $M_{OVT} - \theta_{ST}$ curves for KBA- and KBB-series shown in Fig. 4-3 and 4-4, respectively, clearly show the definite influence of the magnitudes of plastic moments upon the energy capacities. An $M_{OVT} - \theta_{ST}$ curve for a frame with greater plastic moments attains a higher maximum as it should, but it is interesting to observe that the almost flat portion up to the last hinge point increases almost proportionally to the magnitude of plastic moments. Again, the influence of load distributions is only slightly observed.

The increase in the stiffness of the ground floor beam has a slight influence only upon the initial elastic and elastic-plastic response, no influence being observed upon the almost flat portion and the last hinge point as seen in Fig. 4-5. The increase in the plastic moment of the ground floor beam result in a correspondingly higher $M_{OVT} - \theta_{ST}$ curve as may be seen in Fig. 4-6.

In contrast to those for KAA-series, the $M_{OVT} - \theta_{ST}$ curves for UAA-series do not show significant increase in the maximum of M_{OVT} even if the rate of tapering is greater (Fig. 4-7), and have no portion with a negative slope up to the last hinge points. In UBA-series where the plastic moments are uniformly greater, the same tendency as in KBA-series is clearly observed (Fig. 4-8).

5.3 $\theta_p - \theta_{ST}$ curves

In order that the $M_{OVT} - \theta_{ST}$ curve of a frame really represents its response curve, it must be confirmed that the amount of plastic hinge rotations do not exceed their respective rotation capacities before the last hinge point is reached. Otherwise, the rotation capacities limit the extent of validity of the $M_{OVT} - \theta_{ST}$ curve. As soon as the rotation capacities of the members of a frame are determined from the structural details in which stiffeners and lateral constraints to prevent local and lateral buckling are to be inserted in order to extend the rotation capacities, $\theta_p - \theta_{ST}$ curves may be used to determine the limit of allowable horizontal displacement for the frame, although non-structural components may also restrict the limit. It is then possible to define and compute the total energy capacity for the frame.

Fig. 5-1-8 show $\theta_p - \theta_{ST}$ curves for those plastic hinges which attain their respective maxima at their respective last hinge point states. It is observed that all the $\theta_p - \theta_{ST}$ relations may roughly be regarded as linear. As may be observed from Fig. 5-1 and 5-2, a greater plastic hinge rotation capacity is necessary in order that a frame with a smaller rate of tapering in the stiffnesses and plastic moments of beams is able to attain its last hinge point state. The rate of growth of θ_p is greater for a frame with a smaller rate of tapering. This indicates, together with the $M_{OVT} - \theta_{ST}$ curves, that the

tapering is indeed desirable for decreasing the necessary rotation capacities for the same value of θ_{ST} .

Fig.5-3 and 5-4 show that a frame with greater plastic moments of beams is able to attain its last hinge point only if the beams have correspondingly greater rotation capacities. However, the difference in the allowable limits of θ_{ST} corresponding to the same magnitude of θ_p is rather small. Comparison of Fig.5-3 with Fig.5-4 clearly shows that the magnitudes of hinge rotations required to attain the last hinge point states are considerably less for frames with greater rate of tapering.

The θ_p - θ_{ST} curves for the frames of KAc-series are almost identical (Fig.5-5). In contrast to Fig.5-1-4, the θ_p - θ_{ST} curve for a frame with greater plastic moment of the ground floor beam has a greater rate of growth with respect to θ_{ST} as observed in Fig.5-6. The θ_p - θ_{ST} curves for UAa and UBa frames are similar to those for KAa and KBa frames, respectively. The essential difference between the curves for K-series and for U-series is that the magnitudes of θ_p required to attain their last hinge point states in U-series are about one quarter of the θ_p -values for K-series.

5.4 W_H and W_H'

Fig.6-1-8 show W_H - θ_{ST} curves up to their respective last hinge point states. The last hinge point of a frame does not necessarily set the limit of its energy absorption capacity. An M_{OVT} - θ_{ST} curve for a tall frame has a portion with negative slope even before it attains the last hinge point state. Although such a portion may result in an unstable dynamic response, the static horizontal forces can still do work even during its mechanism state. The energy absorption capacity corresponding to such a portion may be effective only if the frame is to withstand against a shock of one-pulse. In this sense, it is rather difficult to find a definite significance of the last hinge point in defining a total energy absorption capacity, except, of course, that it is a limit of kinematic stability at which the negative slope becomes greater and almost equal to that of a mechanism curve. A more realistic total energy absorption capacity should therefore be defined in terms of an allowable θ_{ST} value as mentioned in the preceding article. Since, however, reliable practical data on the rotation capacities of plastic hinges do not seem to be available at present, W_H as a function of θ_{ST} and the rate of work W_H' are discussed here in details. Henceforth W_H will be called simply the energy absorption capacity.

The essential feature observed through Fig.6-1-8 is that all the W_H - θ_{ST} curves after several plastic hinges have formed are almost linear. The average rate of work done by the horizontal forces, W_H' , which is nothing but a rate representation of the energy absorption capacity is a characteristic constant for a frame. Since θ_p -values are almost proportional to θ_{ST} values as a general tendency, if a definite limit is to be assigned on the allowable θ_{ST} -value for a class of frames, then a frame with a greater W_H' -value is able to absorb a greater amount of energy so far as the equivalent elastic displacement limits are the same.

Whereas the effects of tapering of beam sections and of load distributions on W_H are small in KAa-and KAB-series, the increase in the plastic moments of beams directly raises the corresponding W_H - θ_{ST} curves as may be seen in Fig.6-1-4. Correspondingly, whereas W_H' increases at a small rate with respect to r_T , W_H' is proportional to c_M (Fig.7-1-2). Similarly, the increase in the stiffness of the ground floor beam does not result in any visible change in

$W_H - \theta_{ST}$ curves but the increase in its plastic moment raises $W_H - \theta_{ST}$ curves at a greater rate than the one eleventh of the rate of increase on KBa curves (Fig.6-5,6 and Fig.7-1,2). Fig.6-7,8 and Fig.7-1,2 for UAa- and UBa-series show the same tendencies, respectively, as those of KAa- and KBa-series.

6. CONCLUSION

The present paper has explored and clarified the nature of energy absorption capacities of multi-story frames with relatively strong columns. The following conclusions may be drawn from the present numerical results.

- (1) Frames with relatively strong columns and weak beams exhibit rather stable static responses in the sense that the response curves are essentially of bilinear elastic-perfectly plastic type without portions of large negative slopes. The essential feature apparently seen throughout the figures is that, since $W_H - \theta_{ST}$ curves are almost linear respectively after the formation of several plastic hinges, $M_{OVT} - \theta_{ST}$ curves may roughly be regarded as bilinear elastic-perfectly plastic responses and characterized by the average rate of work done by the horizontal forces which is nothing but an energetic representation of the average strength.
- (2) As the plastic hinge rotation is proportional to the top displacement in a rigid-plastic collapse mechanism, θ_p is almost linear with respect to θ_{ST} . Corresponding to a definite limit determined on the rotation capacities of plastic hinges in a frame, θ_{ST} is also limited. It is therefore meaningful to compare W_H for a value of θ_{ST} .
- (3) A frame with a greater rate of linear tapering in beam sections per story has a greater energy absorption capacity even if the sum of beam plastic moments are the same.
- (4) A frame with greater beam plastic moments has a greater energy absorption capacity. The average rate of energy absorption W_H' is proportional to the magnitude of beam plastic moments, whereas the W_H' -value increases with respect to the rate of tapering r_T at a considerably smaller rate than with respect to the rate of increase c_M in the plastic moments.
- (5) Patterns of horizontal load distributions have only a slight influence upon the energy absorption capacity.
- (6) Five-story frames of two bays exhibit similar behaviors to those of ten-story frames, except that the $M_{OVT} - \theta_{ST}$ curves do not have any portions of even slight negative slopes.

ACKNOWLEDGMENTS

The authors are grateful for the comprehensive suggestions of Professors T. Kobori and R. Minai. The authors would like to thank Mr. T. Fujiwara and other members of Kobori-Minai Laboratories for their kind help in preparing this manuscript. The authors are also indebted to the Computer Center of Kyoto University for the use of KDC II computer.

REFERENCES

1. R. Tanabashi, "Some Considerations on Destructive Elements of Earthquake Gound Motion and Earthquake Resistance of Structures", Journal of the Architectural Institute of Japan, Vol.49, No.599, May 1935
R. Tanabashi, "On the Resistance of Structures to Earthquake Shocks", Memoirs of the College of Engineering, Kyoto Imperial University, Vol.IX, No.4, Kyoto, 1937
2. See for instance, G. W. Housner, "Behavior of Structures during Earthquakes" J. Engineering Mechanics Division, ASCE, Vol.85, No.EM4, pp109-129, Oct,1959
3. T. Kobori and R. Minai, "Aseismic Design Method of Elasto-Plastic Building Structures" Disaster Prevention Research Institute, Kyoto University, Bulletin No.68, March 1964
4. S. Ban, R. Tanabashi, T. Kobori, K. Kaneta and H. Muguruma, "The Ultimate Displacement Design Method", Proc. Symposium on the Safety of Structures, pp127-150, Japan National Committee for Bridge and Structural Engineering, Tokyo, 1955
5. Ping-Chun Wang, "Numerical and Matrix Methods in Structural Mechanics", John Wiley & Sons, Inc., 1966
6. M. F. Rubinstein, "Matrix Computer Analysis of Structures", Prentice-Hall, 1966
7. R. Tanabashi and T. Nakamura, "On the Ultimate States of Rigid Frames Subjected to Earthquakes ", Proc. Japan National Symposium on Earthquake Engineering-1962, pp51-56, Tokyo, Japan

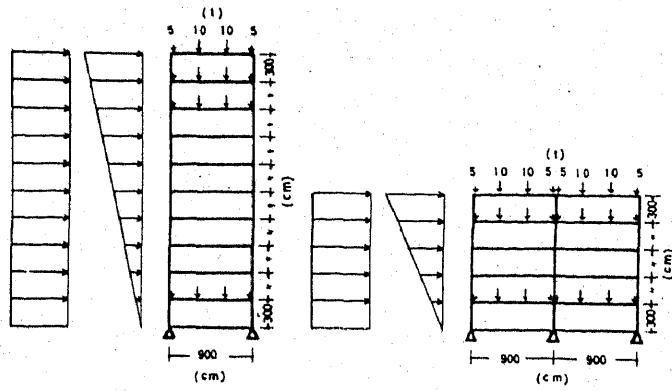


Fig.1 Ten-story frame and five-story frame

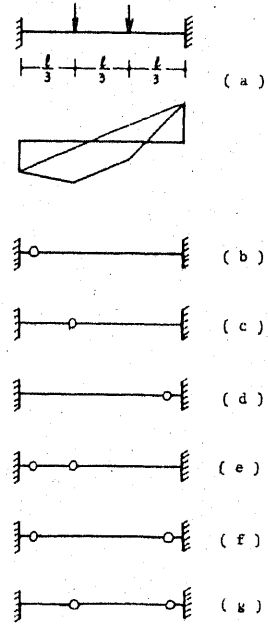


Fig.2 One-hinge patterns and two-hinge patterns

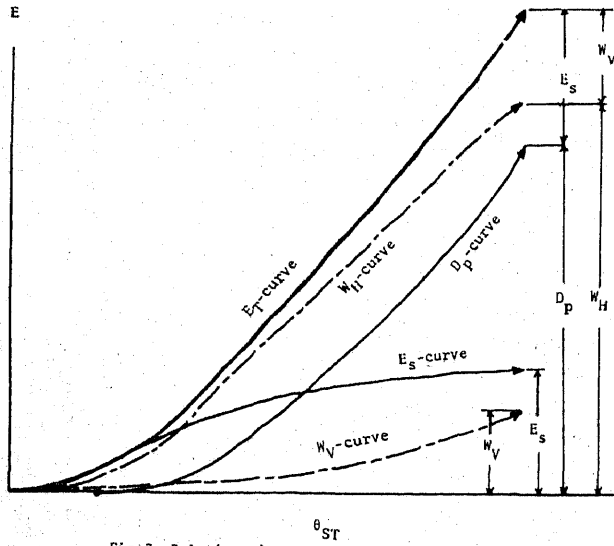


Fig.3 Relations between energy quantities

Table I Structural data

Column Beam $(\bar{I}_C^K / \bar{I}_B^K) / (\bar{I}_C^U / \bar{I}_B^U) = 6.0, (\bar{I}_C^U / \bar{I}_C^K) / (\bar{I}_B^U / \bar{I}_B^K) = 6.0$

	A : variable rate of tapering in stiffnesses and plastic moments					B : variable plastic moments					
	1	2	3	4	5	1	2	3	4	5	
K	a	KAa-1 r_T 0 T_I 1.535	KAa-2 r_T 1/30 T_I 1.509	KAa-3 r_T 2/30 T_I 1.491	KAa-4 r_T 3/30 T_I 1.486	KAa-5 r_T 4/30 T_I 1.494	c_M 2/4	c_M 3/4	c_M 1	c_M 5/4	c_M 6/4
	b	KAb-1 r_T 0 T_I 1.535	KAb-2 r_T 1/30 T_I 1.511	KAb-3 r_T 2/30 T_I 1.498	KAb-4 r_T 3/30 T_I 1.494	KAb-5 r_T 4/30 T_I 1.502	c_M 2/4	c_M 3/4	c_M 1	c_M 5/4	c_M 6/4
	c	KAc-1 c_{KG} 1/2 T_I 1.581	KAc-2 c_{KG} 1 T_I 1.535	KAc-3 c_{KG} 2 T_I 1.496	KAc-4 c_{KG} 4 T_I 1.467	KAc-5 c_{KG} 8 T_I 1.450	c_{MC} 2/4	c_{MC} 3/4	c_{MC} 1	c_{MC} 5/4	c_{MC} 6/4
U	a	UAa-1 r_T 0 T_I 0.947	UAa-2 r_T 1/30 T_I 0.937	UAa-3 r_T 2/30 T_I 0.931	UAa-4 r_T 3/30 T_I 0.928	UAa-5 r_T 4/30 T_I 0.930	c_M 2/4	c_M 5/4	c_M 1	c_M 5/4	c_M 6/4

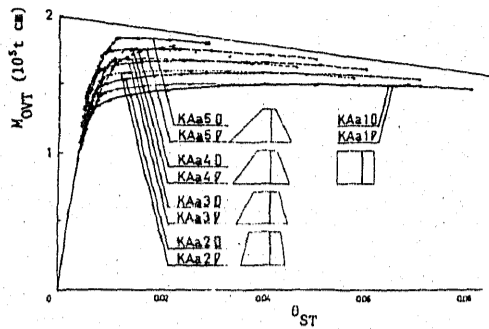


Fig. 4-1(a) $M_{OVT} - \theta_{ST}$ curves for KAA-series

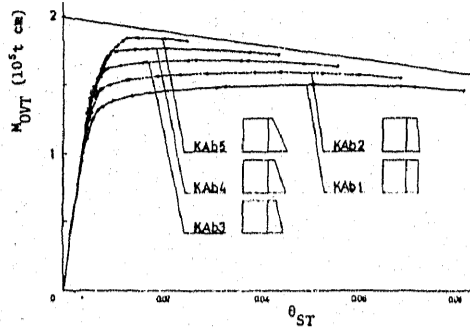


Fig. 4-2(a) $M_{OVT} - \theta_{ST}$ curves for KAB-series

10	20	30	40	50	17	27	37	47	57
25 20	22 20	27 20	27 20	22 1	22 20	22 20	22 20	22 13	21 1
21 19	21 18	21 18	21 18	21 9	21 18	21 18	21 17	21 8	19 1
18 16	19 16	18 16	18 16	20 8	18 16	19 16	19 9	20 9	18 3
17 15	17 15	17 15	17 15	18 8	17 15	17 7	16 7	16 5	14 4
15 11	15 9	15 8	15 8	16 4	15 8	16 5	16 5	14 2	12 5
13 7	13 5	14 4	14 3	14 3	13 5	14 4	13 3	11 1	11 6
12 5	12 4	12 3	12 4	12 1	12 4	12 2	10 1	10 2	12 2
10 2	11 3	10 1	10 2	11 2	10 2	9 1	9 2	12 5	16 6
9 2	8 1	9 2	9 1	12 3	9 1	9 2	11 4	16 7	17 9
8 1	10 2	11 3	11 3	15 10	11 3	12 5	16 6	17 8	20 10
6 3	7 6	8 7	8 7	18 15	9 7	12 11	14 13	19 10	22 11

Fig. 4-1(b) Order of Plastic hinge formation

1	2	3	4	5
22 20	22 20	22 18	22 18	21 1
21 19	21 18	21 18	21 18	22 2
19 16	19 16	20 15	20 15	20 9
17 15	17 15	17 13	18 7	18 6
13 11	15 8	16 6	17 9	16 6
12 7	12 5	14 5	15 5	14 4
12 4	12 4	12 4	12 3	13 3
10 2	11 3	8 2	9 2	11 2
8 1	8 1	7 1	8 1	12 5
6 3	10 2	11 2	11 4	15 10
5 5	7 6	10 8	13 11	17 16

Fig. 4-2(b) Order of plastic hinge formation

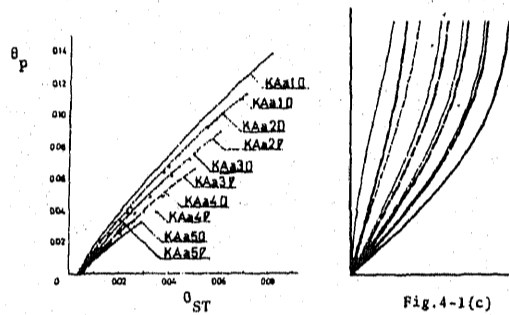


Fig. 5-1 $\theta_p - \theta_{ST}$ curves for KAA-series

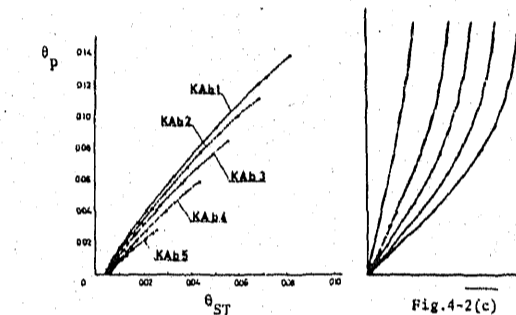


Fig. 5-2 $\theta_p - \theta_{ST}$ curves for KAB-series

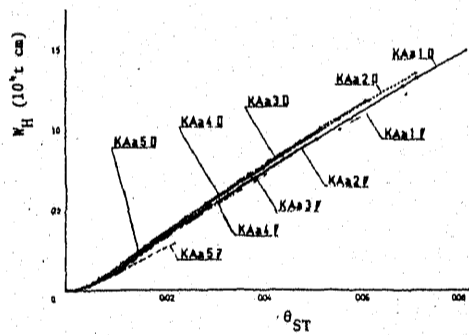


Fig. 6-1 $W_H - \theta_{ST}$ curves for KAA-series

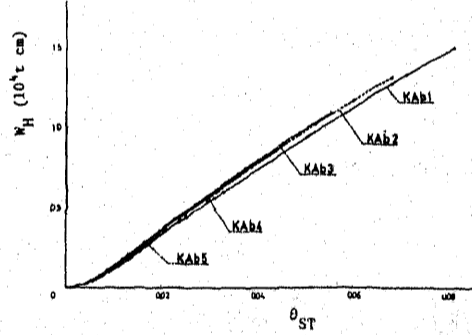


Fig. 6-2 $W_H - \theta_{ST}$ curves for KAB-series

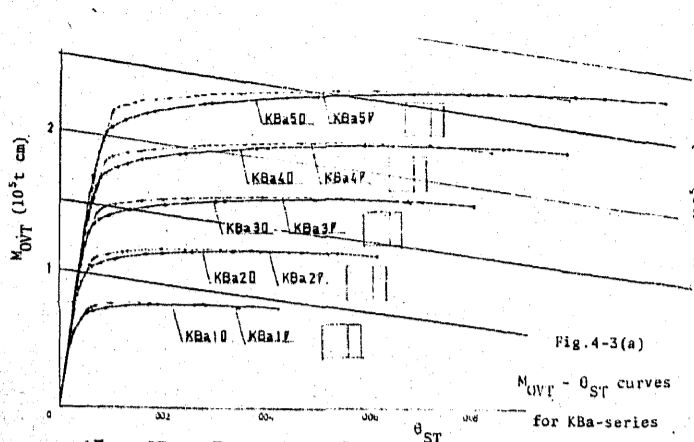


Fig. 4-3(a)

$M_{OVT} - \theta_{ST}$ curves for KBa-series

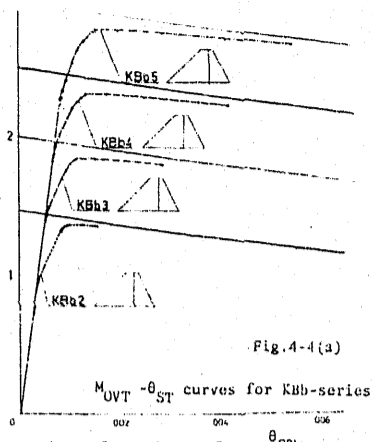


Fig. 4-4(a)

$M_{OVT} - \theta_{ST}$ curves for KBb-series

1□		2□		3□		4□		5□		1▽		2▽		3▽		4▽		5▽			
22	18	27	20	27	20	27	21	27	21	27	29	27	30	27	27	20	27	21	27	21	
21	17	21	18	21	19	20	19	20	19	21	17	21	18	21	18	20	19	20	19	20	19
20	15	15	16	18	16	18	17	18	17	20	15	19	15	19	16	18	15	18	17	18	17
18	9	17	13	17	14	16	14	16	15	16	7	17	9	17	13	15	16	14	16	14	
16	8	15	8	15	11	15	12	14	12	16	6	16	8	15	8	15	6	15	9	8	
14	5	14	5	13	7	13	9	13	10	15	5	14	5	14	5	13	5	13	5	13	5
13	4	13	4	12	4	11	4	11	4	14	4	13	4	12	4	12	4	12	4	12	4
12	3	11	3	10	3	10	3	9	3	12	2	11	2	10	2	10	2	7	2	7	2
11	1	10	2	8	2	8	2	7	2	11	1	10	1	8	1	7	1	6	1	6	1
10	2	8	1	8	1	7	1	8	1	13	3	12	5	11	3	11	2	11	3	11	3
8	7	7	6	6	5	6	5	6	5	9	8	8	7	8	7	9	8	13	9	13	9

Fig. 4-3(b) Order of plastic hinge formation

2		3		4		5	
20	1	27	7	27	10	27	16
22	7	21	5	21	8	21	17
21	5	20	8	22	8	20	5
19	4	19	6	19	6	19	7
18	5	18	4	18	5	15	5
14	6	14	3	14	2	13	4
12	1	13	1	13	1	11	2
11	8	11	7	11	1	8	1
13	9	13	5	12	4	10	3
12	10	15	10	15	7	14	6
16	15	16	17	17	14	16	17

Fig. 4-4(b) Order of plastic hinge formation

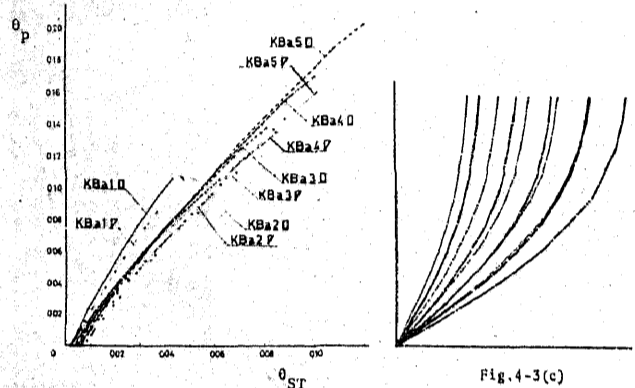


Fig. 5-3

$\theta_p - \theta_{ST}$ curves for KBa-series Modes of Deformation

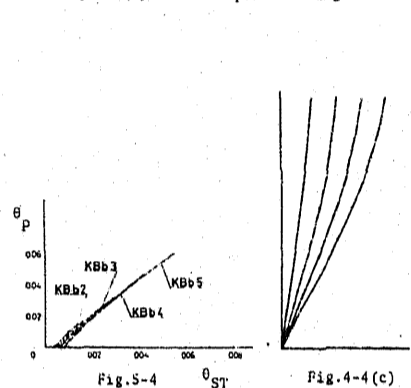


Fig. 5-4

$\theta_p - \theta_{ST}$ curves for KBb-series Modes of Deformation

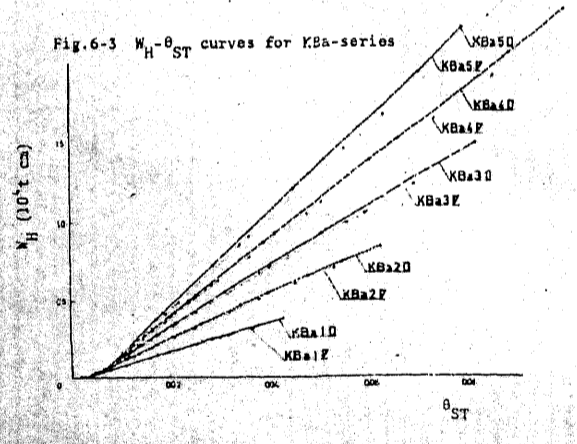


Fig. 6-3 $W_H - \theta_{ST}$ curves for KBa-series

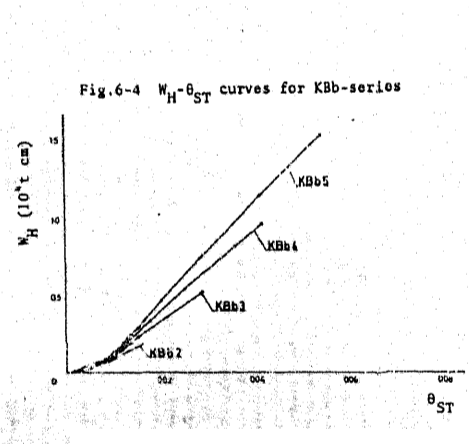


Fig. 6-4 $W_H - \theta_{ST}$ curves for KBb-series

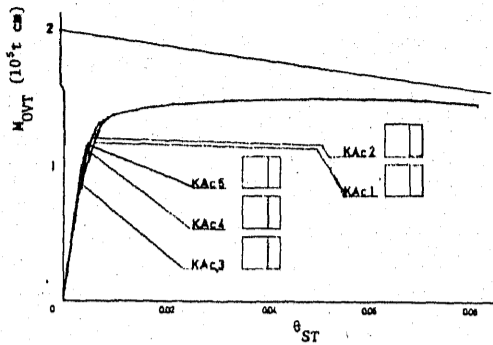


Fig. 4-5(a) $M_{OVT} - \theta_{ST}$ curves for KAc-series

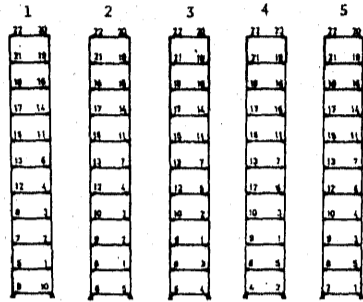


Fig. 4-5(b) Order of plastic hinge formation

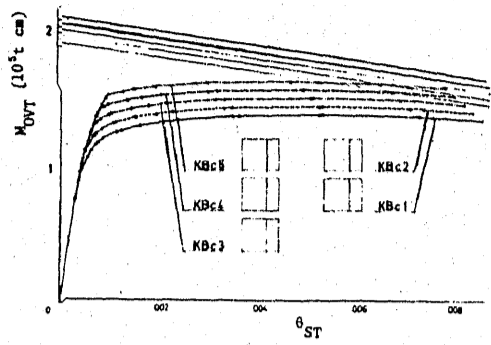


Fig. 4-6(a) $M_{OVT} - \theta_{ST}$ curves for KBc-series

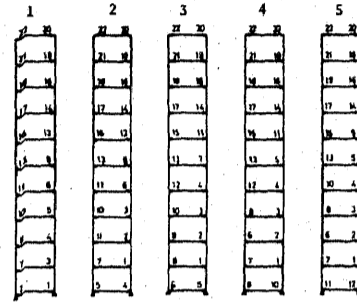


Fig. 4-6(b) Order of plastic hinge formation

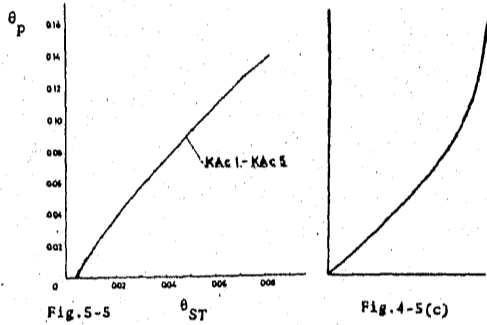


Fig. 5-5 $\theta_p - \theta_{ST}$ curves for KAc-series

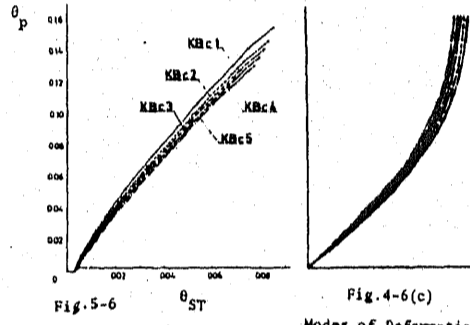


Fig. 4-5(c) Modes of Deformation

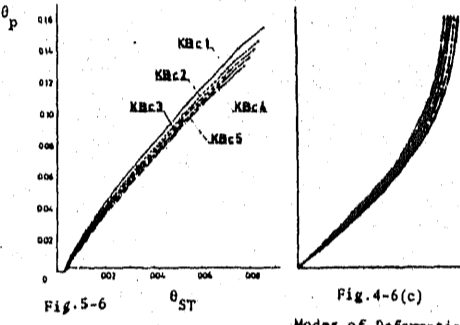


Fig. 5-6 $\theta_p - \theta_{ST}$ curves for KBc-series

Fig. 4-6(c) Modes of Deformation

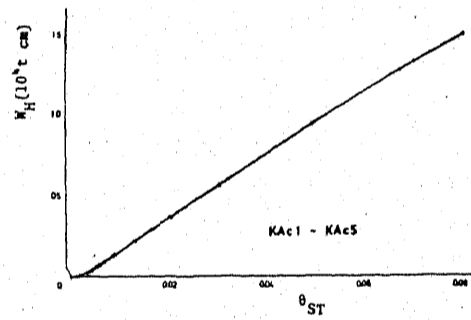


Fig. 6-5 $W_H - \theta_{ST}$ curves for KAc-series

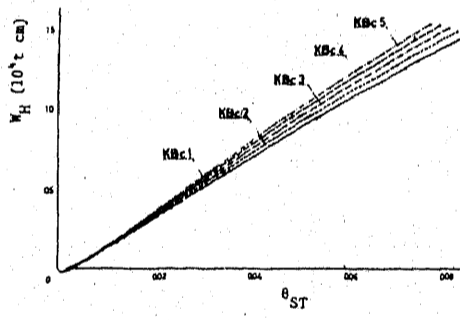


Fig. 6-6 $W_H - \theta_{ST}$ curves for KBc-series

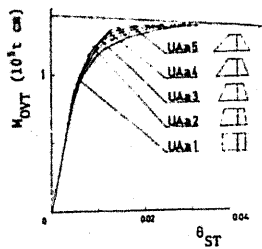


Fig. 4-7(a) $M_{OVT} - \theta_{ST}$ curves for UAA-series

UAA-1	UAA-2	UAA-3	UAA-4	UAA-5
22 17 26 20	23 17 26 20	24 13 21 15	22 8 26 10	21 1 21 4
22 11 21 13	22 11 21 13	22 7 21 8	27 7 21 4	23 2 21 5
19 5 18 4	20 5 18 4	20 5 18 4	20 4 18 4	20 3 19 7
16 7 15 4	16 7 15 4	18 7 17 3	18 1 17 7	16 5 16 8
14 1 13 7	14 1 13 7	16 1 15 4	16 3 15 1	17 9 18 10
20 9 8 7	20 9 8 7	12 11 10 8	14 13 12 11	14 13 12 11

Fig. 4-7(b) Order of plastic hinge formation



Modes of Deformation
Fig. 4-7(c)

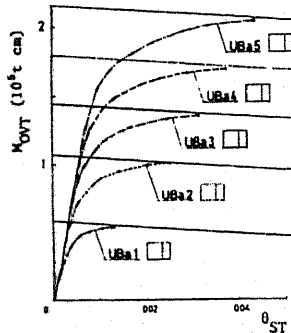


Fig. 4-8(a) $M_{OVT} - \theta_{ST}$ curves for UBA-series

UBA-1	UBA-2	UBA-3	UBA-4	UBA-5
21 9 26 20	23 13 26 20	22 17 26 20	20 18 26 20	21 16 26 20
21 7 22 8	22 11 21 12	22 11 21 12	27 13 21 14	27 15 21 14
18 5 20 4	20 5 18 4	18 5 18 4	18 5 17 4	18 5 17 4
17 7 18 4	16 3 17 4	16 3 16 4	15 3 14 4	14 3 13 4
16 1 15 3	15 1 14 3	14 1 13 2	12 1 11 7	12 1 11 7
14 11 17 11	13 9 8 7	10 8 8 7	10 8 8 7	9 8 7 4

Fig. 4-8(b) Order of plastic hinge formation



Modes of Deformation
Fig. 4-8(c)

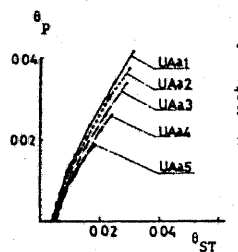


Fig. 5-7 $\theta_p - \theta_{ST}$ curves for UAA-series

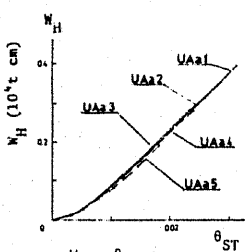


Fig. 6-7 $W_H - \theta_{ST}$ curves for UAA-series

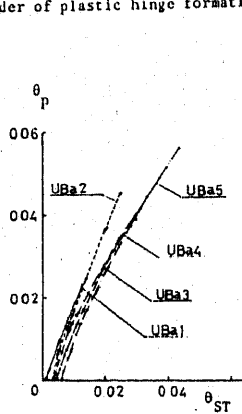


Fig. 5-8 $\theta_p - \theta_{ST}$ curves for UBA-series

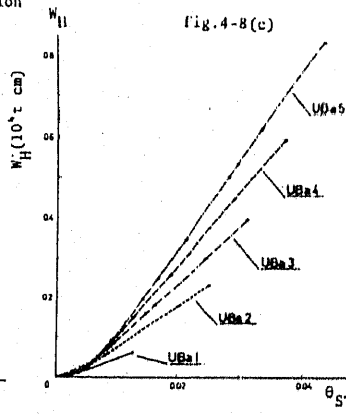


Fig. 6-8 $W_H - \theta_{ST}$ curves for UBA-series

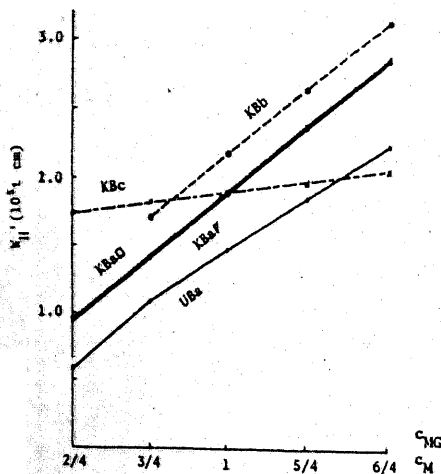


Fig. 7-2 $W_H' - c_M$ curves and $W_H' - c_{MG}$ curve

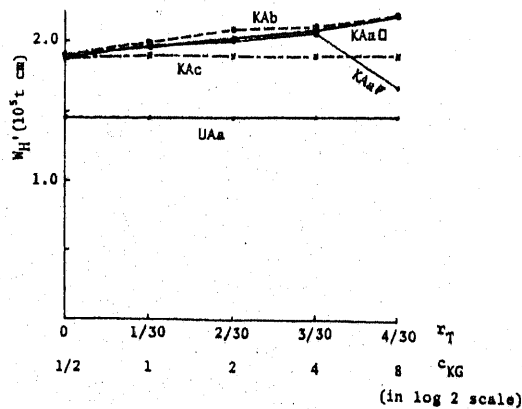


Fig. 7-1 $W_H' - x_T$ curves and $W_H' - c_{KG}$ curve